Rapid Communications

# Spatial analog of the two-frequency torus breakup in a nonlinear system of reactive miscible fluids

Dmitry Bratsun
*Department of Applied Physics, Perm National Research Polytechnical University, Perm 614990, Russia*

(Received 5 June 2019; revised manuscript received 28 July 2019; published 18 September 2019)

We present a theoretical study on pattern formation occurring in miscible fluids reacting by a second-order reaction $A + B \rightarrow C$ in a vertical Hele-Shaw cell under constant gravity. We have recently reported that the concentration-dependent diffusion of species coupled with a frontal neutralization reaction can produce a multilayer system where low-density depleted zones could be embedded between the denser layers. This leads to the excitation of chemoconvective modes spatially separated from each other by a motionless fluid. In this Rapid Communication, we show that the layers can interact via a diffusion mechanism. Since diffusively coupled instabilities initially have different wavelengths, this causes a long-wave modulation of one pattern by another. We have developed a mathematical model which includes a system of reaction-diffusion-convection equations. The linear stability of a transient base state is studied by calculating the growth rate of the Lyapunov exponent for each unstable layer. Numerical simulations supported by phase portrait reconstruction and Fourier spectra calculation have revealed that nonlinear dynamics consistently passes through (i) a perfect spatially periodic system of chemoconvective cells, (ii) a quasiperiodic system of the same cells, and (iii) a disordered fingering structure. We show that in this system, the coordinate codirected to the reaction front paradoxically plays the role of time, time itself acts as a bifurcation parameter, and a complete spatial analog of the two-frequency torus breakup is observed.

DOI: 10.1103/PhysRevE.100.031104

In recent decades, the study of the interaction between reaction-diffusion phenomena and convective instabilities brought many surprises. Let us focus on a neutralization reaction: A second-order $A + B \rightarrow C$ reaction is distinguished by a comparatively simple, albeit nonlinear, kinetics. If two species are initially separated in space, the reaction proceeds in a frontal manner due to the high value of the reaction rate constant. In this case, it may result in various buoyancy-driven instabilities if the reaction occurs either in immiscible two-layer systems [1–5] or in miscible acid-base systems [6–16]. Among the important effects that have been observed here, we highlight the pattern convection in the form of a perfectly periodic system of cellularlike fingers remaining in contact with the interface when an organic solvent containing an acid $A$ is in contact with an aqueous solution of an inorganic base $B$ [3]. At that time, a liquid-liquid interface has been recognized as the main reason for this unusual regularity of salt fingering [2,5]. However, a perfectly organized structure of fingers has been observed already in the miscible system, where two aqueous solutions of base and acid have been brought into contact [13,15]. It was shown that this pattern arises due to the strong dependence of the diffusion coefficients of the initial reactants and the reaction product on their concentrations. The effect of concentration-dependent diffusion (hereinafter CDD) coupled with a fast neutralization reaction has been demonstrated to produce a spatially localized zone with unstable density stratification (figuratively, a density pocket) in a system with an inherently stable configuration, when a less dense solution is placed above a more dense one. It should be noted that such an effect creates a new situation in fluid mechanics when the convective modes arise in different parts of the medium and compete on the distance. In this case, the patterns can be coupled by the diffusion of heat or matter which transmits a signal through an interlayer of the motionless fluid.

Generally, the CDD effect means a significant expansion of the degrees of freedom for the system to produce various types of instabilities and nonlinear dynamics that do not fit into the traditional classification [14]. For example, we have shown recently that when varying initial concentrations of solutions, the density pocket may collapse suddenly, causing a density shock wave separating the fluid at rest and the area with anomalously intense convective mixing [16].

In this Rapid Communication, we study the nonlinear interaction between two periodic systems of chemoconvective cells that arise independently inside two different layers low in density. Although initially the layers are separated by the motionless fluid, they can nevertheless influence each other via the mechanism of the nonlinear diffusion of the reactants. Thus, this configuration reproduces the conditions for the realization of a spatial analog of the two-frequency torus. As it is known, Ruelle and Takens mathematically showed that quasiperiodicity is not generic when nonlinearities are acting [17]. The Ruelle-Takens-Newhouse theory [17,18] postulates that the strange attractor replaces the torus in the phase space after a finite number of bifurcations. In our case, we demonstrate that a similar transition is reproduced, but the role of time is played by the spatial horizontal coordinate with time itself now being a control parameter.

*Mathematical model*. We consider two aqueous solutions of acid $A$ and base $B$ filling the cavity, which is strongly compressed in one of directions, so that the Hele-Shaw (HS) approximation is applied. Right after the process starts, the reagents with initial concentrations $A_0, B_0$ diffuse into each

 

other and are neutralized at a rate $k$ with the formation of salt $C$. Since both reagents are dissolved in water, their mixing begins at the contact of initially separated layers. It is noteworthy that the problem is nonautonomous because reagents are not replenished during the reaction and concentration profiles change irreversibly. Generally, a neutralization reaction is known to be exothermic. However, in this Rapid Communication, the heat release is neglected. In experiments, one can always achieve such reaction conditions, if the walls of the HS cell are made quite conductive for heat to dissipate. In what follows, we assume that $A_0 = B_0$.

The system geometry is given by a two-dimensional domain defined by $0 \leqslant x \leqslant L$, $-H \leqslant z \leqslant H$ with the $x$ axis directed horizontally and the $z$ axis antidirected to gravity. We scale the problem by using $2d$, $4d^2/D_{a0}$, $D_{a0}/2d$, and $A_0$ as the length, time, velocity, and concentration scales, respectively. $D_{a0}$, $\nu$, $c_p$, and $d$ stand for acid diffusivity (table value), kinematic viscosity, and the HS semigap width.

The mathematical model we develop consists in a set of equations for species coupled to the Navier-Stokes equation written in the HS approximation [13],

$$\Phi + \nabla^2 \Psi = 0, \tag{1}$$

$$\frac{1}{\mathrm{Sc}}\left(\partial_t \Phi + \frac{6}{5} J(\Psi, \Phi)\right) = \nabla^2 \Phi - 12\Phi - \partial_x \rho, \tag{2}$$

$$\partial_t A + J(\Psi, A) = \nabla(D_a \nabla A) - \mathrm{Da}\, AB, \tag{3}$$

$$\partial_t B + J(\Psi, B) = \nabla(D_b \nabla B) - \mathrm{Da}\, AB, \tag{4}$$

$$\partial_t C + J(\Psi, C) = \nabla(D_c \nabla C) + \mathrm{Da}\, AB, \tag{5}$$

$$\rho = \mathrm{Ra}_a A + \mathrm{Ra}_b B + \mathrm{Ra}_c C, \tag{6}$$

where $J(F, P) \equiv \partial_z F \partial_x P - \partial_x F \partial_z P$ stands for the Jacobian determinant. Here, we use a two-field formulation for the motion equation, and introduce the stream function $\Psi$ and vorticity $\Phi$. The diffusion terms in Eqs. (3)–(5) are written in the most general form, allowing the concentration-dependent phenomena [19]. The problem involves the following dimensionless parameters,

$$\mathrm{Sc} = \frac{\nu}{D_{a0}}, \quad \mathrm{Da} = \frac{4kA_0 d^2}{D_{a0}}, \quad \mathrm{Ra}_i = \frac{8g\beta_i A_0 d^3}{\nu D_{a0}}, \tag{7}$$

which are the Schmidt number, the Damköhler number, and the set of solutal Rayleigh numbers, where $i = \{a, b, c\}$, respectively. Equations (1)–(6) should be supplemented by the boundary conditions

$$\begin{aligned} &x = 0, L: \quad \Psi = \partial_x \Psi = 0, \quad \partial_x A = 0, \quad \partial_x B = 0, \quad \partial_x C = 0, \\ &z = \pm H: \quad \Psi = \partial_z \Psi = 0, \quad \partial_z A = 0, \quad \partial_z B = 0, \quad \partial_z C = 0, \end{aligned} \tag{8}$$

and the initial conditions at $t = 0$,

$$\begin{aligned} &z \leqslant 0: \quad \Psi = 0, \quad A = 0, \quad B = 1, \\ &z > 0: \quad \Psi = 0, \quad A = 1, \quad B = 0. \end{aligned} \tag{9}$$

We have shown in Refs. [13,15] that the coupling between a second-order reaction and nonlinear diffusion can transform an initially stably stratified fluid layer to a multilayered system

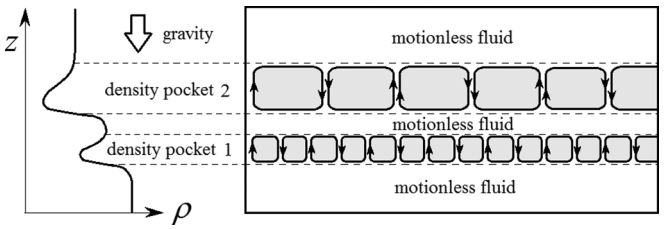


FIG. 1. Schematic presentation of two systems of convective rolls independently arising in a depleted zone low in density.

where the depleted zones low in density are embedded between the denser layers. This situation is presented schematically in Fig. 1. The figure shows a vertical density profile with two local minima, which can be defined as low-density pockets. It is important to note that the fluid layer shown in Fig. 1 remains globally stable, since locally unstable fluid sublayers are not able to set in motion the adjacent immobile fluid. By changing the type of chemical reaction, the involved reagents, or their initial concentrations, we can create quite diverse configurations of the vertical stratification of the system. In order to proceed further, it is necessary to specify the closed-form exact laws of diffusion in (3)–(5). The problem is that so far the CDD effect has been underestimated in fluid mechanics. Therefore, data on the concentration dependence of the diffusion coefficients have appeared to be fragmentary and incomplete for most substances.

Generally, the CDD effect can be observed in ionic systems, and the diffusion of ions depends on the concentration gradient of all ions present. Here, we assume that the diffusion coefficient of each species depends solely on the concentration of this species itself, as if it diffused in a single-component solution. In part, this assumption is based on the consideration of only weak solutions with a concentration of not higher than 3 mol/l, as well as a good agreement of the theory with our experimental observations [13,15]. In fact, at the moment, we have found experimentally the development of the CDD convection for the homologous series of hydroxides of Na, K, Li, and Cs, as well as for a number of acids. We believe that the discovered effect is of a general nature and should be taken into account in reaction-diffusion-convection problems. The specific pair of reagents, $HNO_3$ and NaOH, which we consider in this Rapid Communication is used only because there is a well-developed and experimentally proven model of nonlinear diffusion for these species. Thus, in what follows we use the diffusion laws developed recently for the pair $HNO_3$ and NaOH (for more details, see Ref. [13]),

$$\begin{aligned} D_a(A) &\approx 0.881 + 0.158A, \\ D_b(B) &\approx 0.594 - 0.087B, \\ D_c(C) &\approx 0.478 - 0.284C. \end{aligned} \tag{10}$$

The values of the parameters (7) for the pair $HNO_3$ and NaOH can be estimated as follows: $\mathrm{Sc} = 317$, $\mathrm{Da} = 10^3$, $\mathrm{Ra}_a = 3.2 \times 10^5$, $\mathrm{Ra}_b = 3.8 \times 10^5$, $\mathrm{Ra}_c = 5.1 \times 10^5$.

*Dynamics of the base state and its stability*. The system of equations (1)–(10) allows the base state that describes the dynamics of pure reaction-diffusion processes. In this state, the fluid is at rest all the time. We assume that the fluid

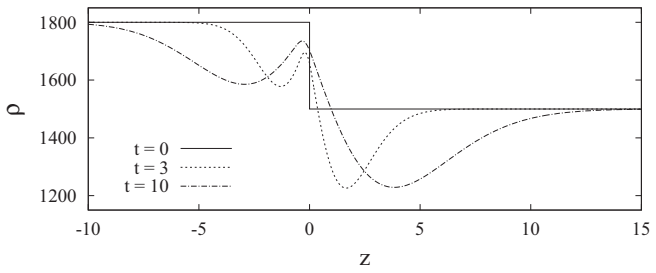


FIG. 2. Instantaneous base state profiles of the density $\rho$ are plotted against the vertical axis $z$ at times $t = 0, 3, 10$.

velocity is zero and concentration fields depend only on the vertical coordinate $z$ and time $t$: $A_0(t,z)$, $B_0(t,z)$, $C_0(t,z)$. Then we obtain

$$\begin{aligned}
\partial_t A_0 &= D_a(A_0)\partial_{zz}A_0 + \partial_z D_a(A_0)\partial_z A_0 - \mathrm{Da}\, A_0 B_0,\\
\partial_t B_0 &= D_b(B_0)\partial_{zz}B_0 + \partial_z D_b(B_0)\partial_z B_0 - \mathrm{Da}\, A_0 B_0,\\
\partial_t C_0 &= D_c(C_0)\partial_{zz}C_0 + \partial_z D_c(C_0)\partial_z C_0 + \mathrm{Da}\, A_0 B_0.
\end{aligned} \tag{11}$$

The problem (8)–(11) can be solved only numerically.

Figure 2 shows the base state profiles of the density $\rho(t,z)$ defined by (6) for three consecutive times $t = 0, 3, 10$. The system starts to evolve from the initial state, in which the lighter acid solution ($z \geqslant 0$) is above the more dense base solution ($z < 0$). Thus, there exists a stable vertical stratification in terms of density, which excludes the development of Rayleigh-Taylor instability. As soon as the reaction-diffusion processes begin, the density profile undergoes dramatic changes: Now it has two minima located above and below the reaction front, implying a possible development of local instabilities in the depleted zones low in density. Thus, the formal scheme shown in Fig. 1 is reproduced in practice. The mechanism of the formation of such a multilayered system has been discussed in detail in Refs. [13,15]. Here, we just briefly note that the main reason is that the reaction product starts to be deposited near the reaction front. Since the diffusion coefficient of salt decreases with the growth of its concentration (the CDD effect), it can progressively accumulate near the reaction front, making a local maximum in the density profile (Fig. 2, $t = 3$). Since the acid has a higher value of the diffusion coefficient, over time, this maximum slowly shifts down (Fig. 2, $t = 10$). Thus, the diffusion makes the system nonautonomous, and time is the control parameter of the system.

Let us analyze the stability of a time-dependent base state defined by Eqs. (10) and (11) with respect to small monotonic perturbations,

$$\begin{pmatrix} \Phi(t,x,z)\\ \Psi(t,x,z)\\ A(t,x,z)\\ B(t,x,z)\\ C(t,x,z)\end{pmatrix} = \begin{pmatrix} 0\\ 0\\ A_0(t,z)\\ B_0(t,z)\\ C_0(t,z)\end{pmatrix} + \begin{pmatrix} \varphi(t,z)\\ \psi(t,z)\\ a(t,z)\\ b(t,z)\\ c(t,z)\end{pmatrix} e^{Ikx}, \tag{12}$$

where $\varphi$, $\psi$, $a$, $b$, $c$ are, respectively, the amplitudes of normal mode perturbations for the vorticity, stream function, acid, base, and salt concentrations, while $k$ is their wave number. Substituting (12) into Eqs. (1)–(6) and linearizing these equations near the base state (11), we obtain the following system of time-dependent amplitude equations for the determination of critical perturbations:

$$\begin{aligned}
\varphi + \partial_{zz}\psi - k^2\psi &= 0,\\
\frac{1}{\mathrm{Sc}}\partial_t\varphi &= \partial_{zz}\varphi - (k^2+12)\varphi\\
&\quad - k^2(\mathrm{Ra}_a\, a + \mathrm{Ra}_b\, b + \mathrm{Ra}_c\, c),\\
\partial_t a &= D_a(A_0)(\partial_{zz}a - k^2 a)\\
&\quad + D_a'(2\partial_z A_0\partial_z a + a\partial_{zz}A_0)\\
&\quad - \mathrm{Da}(A_0 b + aB_0) - \psi\partial_z A_0,\\
\partial_t b &= D_b(B_0)(\partial_{zz}b - k^2 b)\\
&\quad + D_b'(2\partial_z B_0\partial_z b + b\partial_{zz}B_0)\\
&\quad - \mathrm{Da}(A_0 b + aB_0) - \psi\partial_z B_0,\\
\partial_t c &= D_c(C_0)(\partial_{zz}c - k^2 c)\\
&\quad + D_c'(2\partial_z C_0\partial_z c + c\partial_{zz}C_0)\\
&\quad + \mathrm{Da}(A_0 b + aB_0) - \psi\partial_z C_0,
\end{aligned} \tag{13}$$

where the linearization is carried out by taking into account the explicit form of the diffusion laws (10).

Generally, there are two main methods of the linear stability analysis developed for the case when the base state of a hydrodynamic system nonperiodically evolves over time: These are the quasi-steady-state approximation (QSSA) method and the initial value problem (IVP) method. It was shown in Ref. [20] that, excluding short times, there is good agreement between these two approaches. The difference between the methods is that at the very beginning of evolution, the growth rate of disturbances within the IVP calculations is always negative, because the development of the instability takes time. In our case, the system becomes unstable only after some critical period of time and the IVP usage is reasonable [2].

Thus, Eqs. (13) are numerically integrated together with the base state problem (8)–(11) and the boundary conditions for disturbances,

$$z = \pm H: \quad \phi = 0, \quad \partial_z a = 0, \quad \partial_z b = 0, \quad \partial_z c = 0, \tag{14}$$

to compute the growth rate $\lambda$ defined very similarly to the Lyapunov exponent,

$$\lambda(t) = \frac{1}{N}\sum_{j=1}^{N}\frac{1}{\Delta t}\ln\frac{a_j(t+\Delta t, z_{\min})}{a_j(t, z_{\min})}, \tag{15}$$

where $\Delta t$ is the integration time step and $N$ is the number of independent realizations (typically 10–15). Because the growth rate $\lambda$ is sensitive to the given initial data, each independent integration started from white noise with an amplitude of less than $10^{-4}$. We have fixed the occurrence of instability to the time when $\lambda(t)$ averaged over $N$ realizations changes sign from negative to positive. The position $z_{\min}$ for measuring $\lambda$ was chosen at one of the local minima shown in Fig. 2. The integration time step was not constant and changed in accordance with the Courant rule so that the explicit scheme would be stable. Since the final result should be averaged over several runs with random initial conditions, the final growth rate (15) does not depend on the time step.

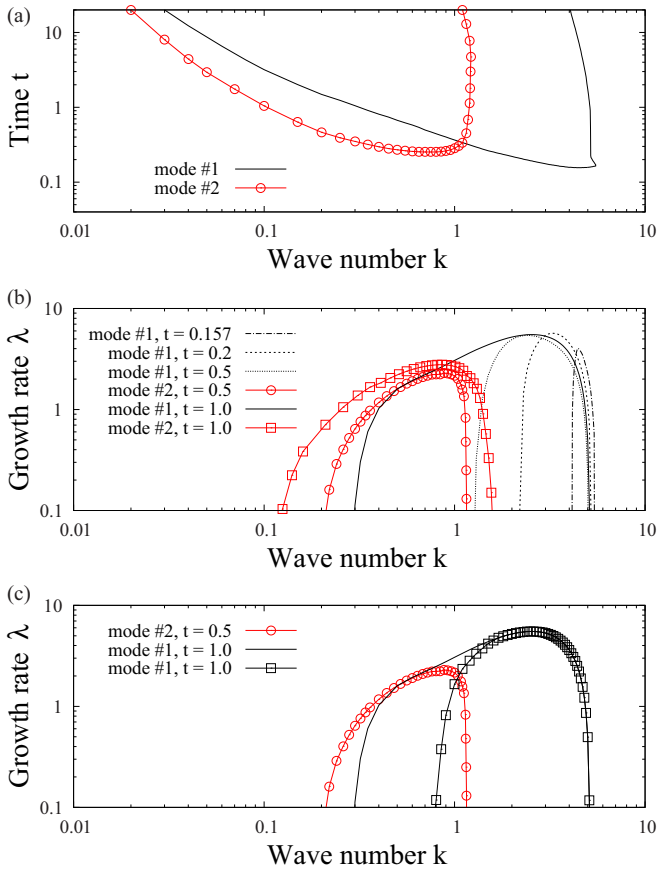


FIG. 3. (a) Neutral curves for two instabilities which arise in two zones low in density shown in Fig. 2. (b) Real part of the growth rate of modes 1 (lines) and 2 (line points) are illustrated at different times. (c) Real part of the growth rate of modes 1 (black line and line points) and 2 (red line points) demonstrates the coupling between modes. The line points indicated by open squares have been calculated for the case when only mode 1 develops in the system, while mode 2 has been artificially suppressed. The same growth rate curve calculated by taking into account the presence of both modes is indicated by the solid line.

Figure 3(a) presents neutral curves for two instabilities which arise independently. Instability 1 below the reaction front (in fact, the CDD instability) develops first. The minimum of the neutral curve corresponds to the wave number $k_1 \approx 4.4$ at time $t_1 \approx 0.156$. Instability 2 starts at $k_2 \approx 0.75$ and $t_2 \approx 0.253$. Figure 3(b) presents the instantaneous growth rates $\lambda$ as a function of $k$ calculated for both instabilities. Although the sublayers are separated by the immobile fluid, the instabilities still can influence each other through a diffusion mechanism [Fig. 3(b), $t = 0.5, 1.0$]. In order to demonstrate clearly the mode interaction, we have recalculated the growth rate curve for mode 1 at $t = 1.0$ in such a way as to allow only this type of instability to develop, suppressing instability 2. This is done by zeroing disturbances in the spatial domain where mode 2 develops. The curve is indicated by open squares in Fig. 3(c). It is interesting to compare this result with those derived for the case when both modes are present [it is indicated by the solid line in Fig. 3(c)]. One can see that the instability region has significantly expanded due to the longer modes. Mode 2 develops exactly in the same wavelength range. The curve of the growth rate for mode 2 is shown for a bit earlier time $t = 0.5$ by taking into account the time delay in the signal transmission, which is explained by slow diffusion. So, the influence of instability 2 on instability 1 looks obvious. It is provided by a relatively mobile acid which easily penetrates the diffusive zone and invades the spatial domain of mode 1. Thus, it is the acid flow that is responsible for the nonlinear coupling between modes. To be precise, the upper mode 2 develops almost independently, since the low-mobile salt and base cannot penetrate the diffusive zone separating the sublayers.

One can see that at times $t > 0.5$, the lower instability 1 can no longer develop independently: Its range of unstable waves expands dramatically due to longer waves, which can be explained by the influence of instability 2 developing in the same range of long waves. Figure 3 demonstrates also that the wavelength ratio of the fastest growing disturbances varies with time, both due to the diffusive expansion of the density pockets and their mutual influence.

*Nonlinear dynamics*. We now discuss the results of the direct numerical simulation of the problem (1)–(10). To see a nonlinear development of the disturbances, the problem has been solved numerically by a finite-difference method (for more details, see Ref. [15]).

We have performed calculations on grids $100 \times 201$ ($L = 20$), $150 \times 201$ ($L = 30$), $300 \times 201$ ($L = 60$), and $625 \times 201$ ($L = 125$), each time keeping the vertical resolution constant ($H = 20$) and consistently increasing the number of nodes in the horizontal direction so as to apply the fast Fourier transform (FFT) algorithm with 64, 128, 256, and 512 data points, respectively. Since the numerical simulations are carried out with the boundary conditions (8), which exclude the imposed periodicity of the resulting structure, the edge effects must be removed from the signal before applying the FFT. At each iteration, one could observe an obvious improvement in the resolution of the Fourier spectrum. Since the main goal was to obtain a clear spectrum for a quasiperiodic signal, the grid resolution $625 \times 201$ was considered sufficient (see below). As the initial condition, we use a random field of the stream function with an amplitude of less than $10^{-3}$.

The nonlinear evolution of the system can be best understood when studying the changes in the terms of the density given by (6). Figure 4 shows a consecutive restructuring of the density field over time. At the very beginning, the base state is absolutely stable, and the fluid convection is absent (Fig. 4, $t = 0.1$). However, two zones of low density are already clearly visible in the figure. The instability in the lower band is excited first. The pattern is a perfectly periodic system of chemoconvective cells enclosed between layers of the motionless fluid (Fig. 4, $t = 0.5$). At this point in time, the wave number of the structure is about $k_1 \approx 2.46$, which agrees well with the linear stability analysis (see Fig. 3). Then, instability 2 is excited in the upper density pocket. The wave number of this structure is much smaller: $k_2 \approx 0.5$ (Fig. 4, $t = 5$). When the latter instability develops sufficiently, it starts to affect the chemoconvection in the lower-density pocket by injecting fresh acid with a spatial periodicity of $2\pi/k_2$. This leads to the formation of an obvious spatial quasiperiodic pattern below the reaction front (Fig. 4, $t = 5$ and 10).

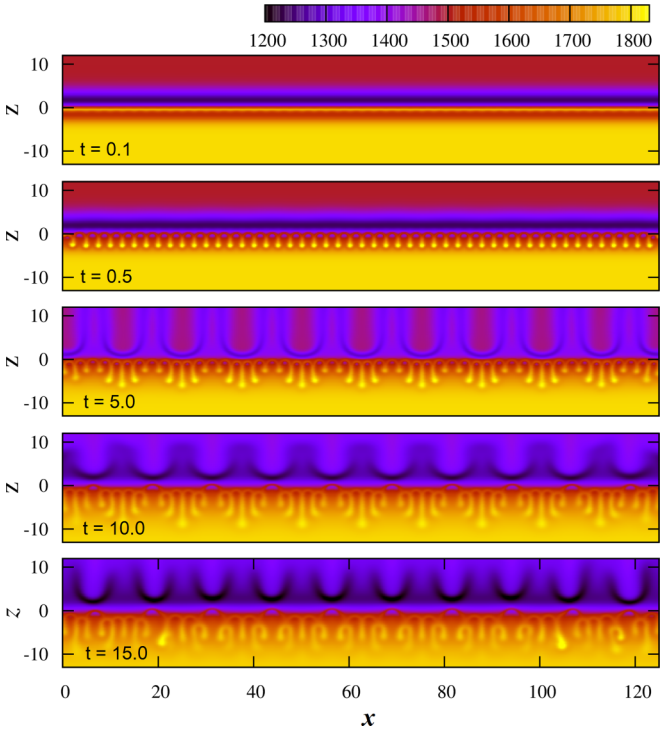


FIG. 4. Nonlinear evolution of the total density $\rho$ with time. The frames from up to down pertain to times $t = 0.1$, 0.5, 5, 10, and 15, respectively. The domain of integration is $0 \leqslant x \leqslant 125$, $-20 \leqslant z \leqslant 20$.

Finally, the pattern loses its regularity and is destroyed (Fig. 4, $t = 15$).

Let us define the coordinate $x$ as a new effective time and consider the "dynamics" of the system. In addition to calculating the power spectrum, we perform the technique of phase portrait reconstruction including the method of delays [21] with preprocessing using the singular value decomposition (SVD) method [22]. In this technique, a multidimensional embedding space is constructed from the time series data. The usage of the SVD method allows calculating an optimal basis for the projection of the reconstructed phase dynamics of the system. In our case, this analysis can be carried out only for a limited number of points equal to the number of grid nodes along $x$ (in fact, even less than 625 grid points taking into account the edge effects). The signal for such an analysis was prepared as follows. The density field $\rho(t, x, z)$ has been spatially averaged across the lower instability band,

$$\hat{\rho}(t, x) = \frac{1}{H_{\text{bot}}} \int_{-H_{\text{bot}}}^{0} \rho(t, x, z) dz, \tag{16}$$

to yield the averaged profile $\hat{\rho}(t, x)$ depending on time $t$ being the governing parameter and the longitudinal coordinate $x$ playing the role of effective time. Here, $H_{\text{bot}}$ stands for the width of the lower instability zone.

Figure 5 shows the Fourier spectra and phase portrait reconstructions calculated for three characteristic points in time. The dynamic mode in Fig. 5, $t = 0.5$, can be unambiguously characterized as periodic. The first peak of the power spectrum determines the authentic wave number of

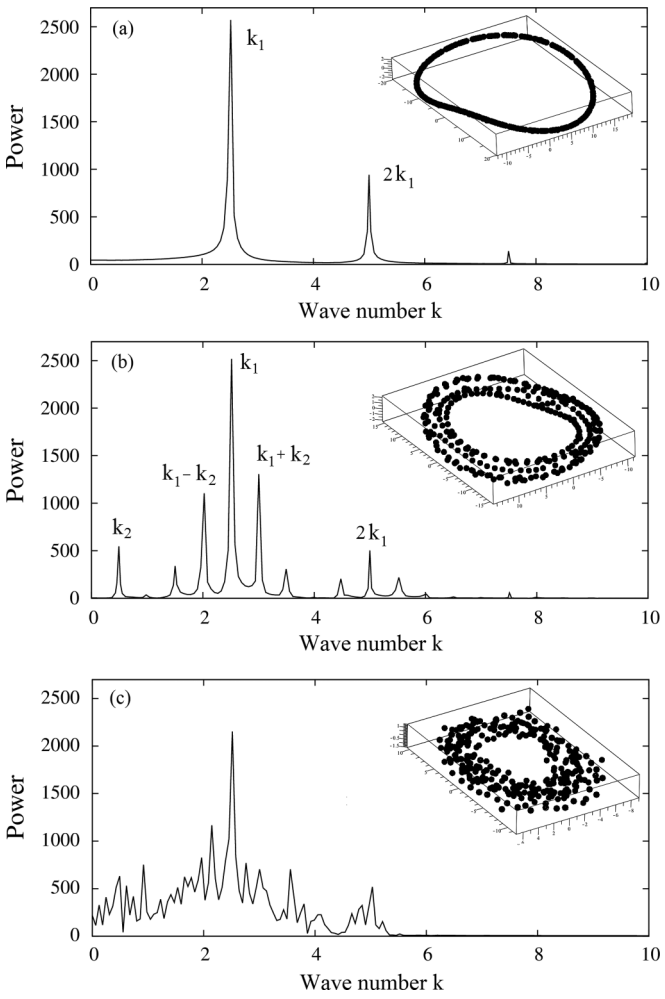


FIG. 5. The power spectra and phase portraits (in the inset) reconstructed from the averaged density $\hat{\rho}(t, x)$ at three consecutive times: (a) $t = 0.5$, (b) $t = 5$, and (c) $t = 15$.

the first instability $k_1 \approx 2.46$, and the second one is simply the double value of the first peak. Thus, the transition from a stable base state (Fig. 4, $t = 0.1$) to a periodic system of chemoconvective cells (Fig. 4, $t = 0.5$) can be interpreted as a spatial Hopf bifurcation giving rise to a limit cycle shown in the inset of Fig. 5. The following dynamic mode demonstrates obvious signs of a quasiperiodic behavior (Fig. 5, $t = 5$). The effect of instability 2 is expressed in the fact that the power spectrum now contains two characteristic peaks and all other peaks are just their linear combinations. The peak in the long-wave part of the spectrum corresponds to the wave number $k_2 \approx 0.5$. Thus, the transition from the periodic cells (Fig. 4, $t = 0.5$) to a spatially quasiperiodic system of chemoconvective cells (Fig. 4, $t = 5$) can be interpreted as a secondary Hopf bifurcation giving rise to a two-dimensional torus shown in the inset of Fig. 5, $t = 5$. Since the "time series" based on $\hat{\rho}(t, x)$ is insufficient for studying the complex bifurcations that require long data sequences, we cannot assert whether another Hopf bifurcation to a three-dimensional torus is occurring reliably. But we can insist that the torus eventually collapses, giving way to a toroidal strange

attractor (Fig. 4, $t = 15$). Here, the spectrum contains already continuous ranges of the excited waves characteristic of chaotic behavior.

*Discussion and closing remarks*. As it is well known, the Ruelle-Takens-Newhouse theory states that an arbitrarily small perturbation of a quasiperiodic flow on the three-dimensional (3D) torus can lead to the stochastic regime of deterministic chaos characterized by long-term unpredictability due to sensitivity to initial conditions, i.e., the strange attractor. Thus, they have showed that quasiperiodicity is not generic when nonlinearities are acting and the transition occurs only after a finite and small number of bifurcations. Notice that the transition from the two-frequency torus to the strange attractor can occur in different ways studied in the special literature on nonlinear dynamics [23]. However, all of these results relate to dynamic systems that evolve over time. In this Rapid Communication, we demonstrate that the scenario of the torus breakup can also be realized if the system evolves over space. This occurs in the physical system of two miscible solutions of $HNO_3$ and NaOH, in which reaction-diffusion-convection processes lead to the appearance of spatially separated chemoconvective instabilities interacting with each other by means of diffusive signals. Since the instability wavelengths are independent parameters, the nonlinear interaction of the two modes leads to the appearance of a spatial quasiperiodic pattern, which is destroyed under the action of nonlinearity and is replaced by the stochastic regime of deterministic chaos characterized by the broadband noise. Since the spatial window within which we can analyze the nonlinear dynamics is limited due to natural reasons, we cannot describe the process of the torus breakup itself in more detail. Any scenario including either a period doubling cascade or the birth of 3D tori requires a significantly longer spatial series in which one basic oscillation should be repeated at least 1000 times. What we have shown in this Rapid Communication that our spatially evolving dynamic system, apparently, displays the breakup of an invariant 2D torus into the strange attractor.

*Acknowledgments.* We gratefully acknowledge the support of this work by the Russian Science Foundation Grant No. 19-11-00133.

[1] K. Eckert and A. Grahn, Phys. Rev. Lett. **82**, 4436 (1999).
[2] D. A. Bratsun and A. De Wit, Phys. Fluids **16**, 1082 (2004).
[3] K. Eckert, M. Acker, and Y. Shi, Phys. Fluids **16**, 385 (2004).
[4] Y. Shi and K. Eckert, Chem. Eng. Sci. **63**, 3560 (2008).
[5] D. A. Bratsun and A. De Wit, Chem. Eng. Sci. **66**, 5723 (2011).
[6] L. Rongy, P. M. J. Trevelyan, and A. De Wit, Phys. Rev. Lett. **101**, 084503 (2008).
[7] A. Zalts, C. El Hasi, D. Rubio, A. Ureña, and A. D'Onofrio, Phys. Rev. E **77**, 015304(R) (2008).
[8] C. Almarcha, P. M. J. Trevelyan, P. Grosfils, and A. De Wit, Phys. Rev. Lett. **104**, 044501 (2010).
[9] K. Tsuji and S. C. Müller, J. Phys. Chem. Lett. **3**, 977 (2012).
[10] S. H. Hejazi and J. Azaiez, J. Fluid Mech. **695**, 439 (2012).
[11] J. Carballido-Landeira, P. M. J. Trevelyan, C. Almarcha, and A. De Wit, Phys. Fluids **25**, 024107 (2013).
[12] M. C. Kim, Chem. Eng. Sci. **112**, 56 (2014).
[13] D. Bratsun, K. Kostarev, A. Mizev, and E. Mosheva, Phys. Rev. E **92**, 011003(R) (2015).
[14] P. M. J. Trevelyan, C. Almarcha, and A. De Wit, Phys. Rev. E **91**, 023001 (2015).
[15] D. A. Bratsun, O. S. Stepkina, K. G. Kostarev, A. I. Mizev, and E. A. Mosheva, Microgravity Sci. Technol. **28**, 575 (2016).
[16] D. Bratsun, A. Mizev, E. Mosheva, and K. Kostarev, Phys. Rev. E **96**, 053106 (2017).
[17] D. Ruelle and F. Takens, Commun. Math. Phys. **20**, 167 (1971).
[18] S. Newhouse, D. Ruelle, and F. Takens, Commun. Math. Phys. **64**, 35 (1978).
[19] J. Crank, *The Mathematics of Diffusion* (Clarendon, Oxford, UK, 1975).
[20] C. T. Tan and G. M. Homsy, Phys. Fluids **29**, 3549 (1986).
[21] N. H. Packard, J. P. Crutchfield, J. D. Farmer, and R. S. Shaw, Phys. Rev. Lett. **45**, 712 (1980).
[22] D. S. Broomhead and G. P. King, Physica D. **20**, 217 (1986).
[23] V. Afraimovich and S.-B. Hsu, *Lectures on Chaotic Dynamical Systems* (International Press, Boston, MA, 2003).